Current distributions of thermal switching in extremely underdamped Josephson junctions

Paolo Silvestrini
Instituto di Cibernetica del Consiglio Nazionale delle Ricerche, Via Toiano 6, 80072 Arco Felice, Napoli, Italy

Olivier Liengme* and K. E. Gray
Materials Science Division, Argonne National Laboratory, Argonne, Illinois 60439
(Received 1 June 1987)

The first measurements of the switching current distribution of an extremely underdamped Josephson junction are presented at various temperatures. Careful fitting of the data provides an experimental verification of the thermal activation theory in the very low damping limit. Moreover, the fitting allows us to obtain the "effective" resistance of a Josephson tunnel junction, thus providing an important indication as to the proper junction resistance to be used in the resistively shunted junction model. These values of junction resistance show the temperature dependence of a subgap resistance, i.e., $\exp(\Delta/k_B T)$, due to activation of quasiparticles over the superconductor energy gap Δ.

I. INTRODUCTION

The effect of noise, both thermal and quantum, on the dynamics of a Josephson junction has received considerable theoretical[1-19] and experimental[20-32] attention in recent years. Such studies are of intrinsic interest and also have technological importance in determining the limits of sensitivity and applicability of devices employing superconducting weak links.

In this report we describe an experimental investigation of the effect of thermal noise on the switching current in an extremely hysteretic Josephson junction (very low damping case). In fact, measurements of this kind have already been performed for higher damping in both the thermal[21,22] and quantum limits,[25,26] by several authors. In the very low damping regime, however, the resistance of the junction should play an important role. The knowledge of such resistance and its temperature dependence, would provide an answer to the important theoretical and practical question of what "effective" junction resistance has to be put in the resistively shunted junction (RSJ) model (note that the resistance of a Josephson junction is not well defined, since the current-voltage characteristic is highly nonlinear in the subgap region). For this reason, an experimental investigation of very low damping junctions has additional interest, since, e.g., it would be very useful in experiments investigating macroscopic quantum tunneling.[13]

The thermal activation model has two parameters, the critical current, I_c, and the effective noise temperature, T_N, in addition to the effective junction resistance discussed above. In principle, T_N should be the bath temperature, T, but externally introduced electrical noise can simulate higher T_N values. Since thermally activated switching causes transitions for a distribution of $I<I_c$, the value of I_c is a limiting value whose magnitude can only be extrapolated from experimental data using such a model. Therefore, for greatest generality, we first fit the model using three free parameters (T_N, I_c, and the effective resistance, R). Since $T_N \sim T$ in this fit, an equally good fit is obtained by assuming $T_N = T$ and leaving the other two parameters free. Similarly, the values of I_c are found to be approximately constant, so we have also fit for the effective junction resistance alone, choosing an average I_c. In this case the fit was somewhat poorer.

In the following we first introduce the problem of thermal induced transitions from the $V=0$ to the $V\neq 0$ state of a Josephson junction from a theoretical point of view, indicating in particular, differences between the two damping regimes in hysteretic junctions. Then we describe the experimental apparatus and show the data taken at different temperatures. Particular care has been taken in fitting the data to theory, e.g., we discuss the statistical compatibility of experimental points with theoretical curves, the errors on the fitting parameters, and their correlations. The temperature dependence of the effective resistance of the junction will be compared with the resistances measured on the I-V characteristics. Finally, the limits of our experimental technique to determine the effective resistance are discussed.

II. THEORETICAL OUTLINE

As is well known, the electrodynamics of a Josephson junction is typically described in terms of an equivalent current-biased circuit consisting of a capacitor C and a resistor R (the "effective resistance" of the junction, which is assumed to be constant) in parallel with a superconductor element (RSJ model). Within this model, the junction equation of motion is a Langevin-like equation of the form

$$\ddot{\theta}+\eta\dot{\theta}+dU/d\theta=\xi(t)\ , \tag{1a}$$

$$\langle\xi(t)\rangle=0,\quad \langle\xi(t)\xi(t')\rangle=\frac{4\eta\omega_j^2}{\gamma}\delta(t-t')\ , \tag{1b}$$

 ©1988 The American Physical Society

where

$$U(\theta)=\omega_j^2(\alpha\theta+\cos\theta)\ .$$

We introduce the dimensionless "temperature" parameter, $\gamma=\hbar I_c/ek_BT$, the "friction" parameter, $\eta=1/RC$, and the plasma frequency, $\omega_j=(2eI_c/\hbar C)^{1/2}$. Here θ is the phase difference across the junction, α is the bias current I measured in units of the critical current I_c (i.e., $\alpha=I/I_c$).

The behavior predicted by Eq. (1) is easily understood in terms of the mechanical analog, i.e., that of a Brownian particle performing its motion in a potential energy $U(\theta)$, with the damping coefficient η and in the presence of the random force $\xi(t)$ where θ is the position of the particle. For $\alpha<1$, $U(\theta)$ shows a series of relative minima (potential wells) separated by a potential energy barrier, U_0, which is a decreasing function of α:

$$U_0=\omega_j^2E,\quad E=-\pi\alpha+2[\alpha\sin^{-1}\alpha+(1-\alpha^2)^{1/2}]\ .$$

For $\alpha=1$ the potential barrier U_0 becomes zero. The $V=0$ state of the junction can be visualized as a particle which is trapped in a well and is performing oscillations around the potential minimum with a frequency $\bar{\omega}=(1-\alpha^2)^{1/4}\omega_j$. The voltage across the junction is related to the speed of the particle by the Josephson relation $V=(\hbar/2e)\dot{\theta}$, so that a nonzero average voltage ($V\neq0$ state) appears when the particle leaves the well and starts running down to the potential slope with an average velocity.

In the absence of noise ($T\to0$ or $\gamma\to\infty$), the system would show a deterministic transition from the $V=0$ to the $V\neq0$ state at $I=I_c$, when the potential barrier U_0 becomes zero. Noise can cause the escape from the potential well even when a barrier is present ($\alpha<1$), and such transitions occur at current values I which are smaller than I_c. This process can be described in terms of a lifetime τ of the $V=0$ state which is metastable against transitions to the $V\neq0$ state. The problem of the escape from a metastable state in the presence of thermal noise has been treated in a pioneering work by Kramers,[33] and in recent years many theoretical works have provided extensions of Kramer's result.[5–11] As is well known, in the Kramer's theory, the expression for the lifetime depends on the value of the dimensionless damping parameter $\epsilon=\eta/\omega_j$. Even in the case of hysteretic junctions ($\epsilon<1$, underdamped case) we have to consider two different regimes: one is the intermediate damping (ID) regime, which is characterized by the lifetime for the $V=0$ state[33]

$$\tau_{\rm ID}=\left[\frac{1}{2\pi}[(\eta/2)^2+(2\pi\bar{\omega})^2-\eta/2]\exp(-\gamma E/2)\right]^{-1}\ . \tag{2}$$

As Kramers pointed out, this formula is only applicable for intermediate values of ϵ, i.e., for $\epsilon\gtrsim(1-\alpha^2)^{1/4}/\pi\gamma E$ [or $\eta/\bar{\omega}\gtrsim(\pi\gamma E)^{-1}$]. However, since $\pi\gamma E\gg1$ in typical experimental situations, the allowed values for the ratio $\eta/\bar{\omega}$ in Eq. (2) may be much less than 1. For the case of $\eta/\bar{\omega}\ll1$, Eq. (2) reduces to

$$\tau_{\rm TR}=\left[\frac{\bar{\omega}}{2\pi}\exp(-\gamma E/2)\right]^{-1}\ . \tag{3}$$

This is the well-known transition-state-method result of calculating the lifetime [transition rate (TR) theory]. The previous experimental work on noise effect in hysteretic junctions has mostly interpreted the data within the ID framework, using Eq. (3) to fit the data. Note that no information on the effective junction resistance can be obtained, since $\tau_{\rm TR}$ is independent of R.

However a change of regime is expected to occur in the Kramer's theory for an extremely underdamped junction. For very small values of the damping parameter ϵ, we are in the very low damping (LD) regime in which the lifetime depends linearly on the effective resistance through the friction parameter, $\eta\equiv(RC)^{-1}$:

$$\tau_{\rm LD}=\frac{1}{\eta}\frac{\exp(\gamma E/2)}{\gamma E/2}=RC\frac{\exp(\gamma E/2)}{\gamma E/2}\ . \tag{4}$$

Following Kramers, we can say that Eq. (4) should be used instead of Eq. (3) if $\tau_{\rm TR}/\tau_{\rm LD}<1$ [i.e., $\eta/\bar{\omega}<(\pi\gamma E)^{-1}$]. Note that this final condition also allows Eq. (4) to be valid for some high damping cases.

Summarizing, in hysteretic junctions ($\epsilon<1$) the lifetime of the $V=0$ state is given by Eq. (2) if $\tau_{\rm TR}>\tau_{\rm LD}$, whereas Eq. (4) must be used if $\tau_{\rm LD}>\tau_{\rm TR}$. In both cases, Kramer's theory assumes $\gamma E/2\gg1$.

In recent years, the Kramer's theory has been generalized[6–9] to provide bridging between these limits over the full damping range. In Ref. 8, for instance, thermal activation in an extremely underdamped junction is investigated for a wide range of damping constants, and the authors obtained an expression for $\tau_{\rm LD}$ which describes the intermediate region [$\eta/\bar{\omega}\sim(\pi\gamma E)^{-1}$] very well and reduces to Kramer's result for $\eta/\bar{\omega}<(\pi\gamma E)^{-1}$. Moreover, the extremely underdamped case has been recently studied to provide an expression for $\tau_{\rm LD}$ which is also valid for small energy barriers ($\gamma E/2\sim1$) and yields Kramer's result for $\gamma E/2\gg1$. Such extensions of Kramer's theory are necessary to account for some experimental situations in Josephson junctions.

In our experiments to test these ideas, the bias current, I, changes as a function of time and switching events are observed at various current values. The resulting distribution function, $P(I)$, is related to the lifetime $\tau(I)$. Since the directly measured quantity is $P(I)$ rather than $\tau(I)$, it is useful to write the well-known relationship between such quantities:[9]

$$P(I)=\left[\frac{dI}{dt}\right]^{-1}\tau^{-1}\exp\left[-\int_0^I\left[\frac{dI}{dt}\right]^{-1}\tau^{-1}(I')dI'\right]\ . \tag{5a}$$

Obviously the same process can be described in terms of the switching time distribution, $P(t)$, as

$$P(t)=\tau^{-1}\exp\left[-\int_0^t\tau^{-1}dt'\right]\ . \tag{5b}$$

Let us observe that the bias current appears in τ as $\alpha=I/I_c$. Therefore in the experiments, care is required to get a good determination of the ratio I/I_c.

III. EXPERIMENT DESCRIPTION

A. Junction fabrication and characterization

The samples used in the experiments were Nb-Nb_xO_y-Pb tunnel junctions prepared by a standard procedure. The base electrode was made by sputtering a Nb film on a Corning glass substrate. The desired geometry was obtained by standard photolithography and chemical etching. A titanium oxide film was deposited between the substrate and the Nb film to avoid etching the glass substrate and possibly breaking the counter electrode. After back sputtering for cleaning, a native-oxide barrier was grown by thermal oxidation in air. A Pb film as counter electrode was then e-beam evaporated and the junction was completed by the second electrode photolithography. The resulting structure was a cross-type, $100\times 50\mu m^2$, Josephson tunnel junction.

The junctions were of good quality, with a sharp rise in the quasiparticle tunnel current at the sum of energy gaps ($\simeq 2.6$ MeV) at $T=4.2$ K, and a low subgap leakage current. A sample with a low critical-current density ($J_c \simeq 2.8$ A/cm^2) was chosen for measurements in order to have an extremely underdamped junction.

The junction capacitance was measured by the Fiske step voltages using the sum of the penetration depths of Pb and Nb determined from the magnetic field diffraction pattern. A value of $C=500\pm 100$ pF was obtained. The critical-current density was uniform, as confirmed by the good diffraction pattern of the critical current in an external magnetic field, with modulation to zero at the minima. The normal resistance of the junction was $R_N=8.0\ \Omega$. A discussion of the behavior of the subgap resistance as a function of the temperature will be given in Sec. IV. We point out that using $R_N=8\ \Omega$ in the RSJ model yields a very low value of the damping parameter ($\epsilon \cong 8.5\times 10^{-3}$; $\beta_c \simeq 13\,500$). The higher, subgap values of resistance yield an even smaller value of ϵ, so we are clearly in the extremely low damping regime of the RSJ model for our experiment (see Sec. IV).

B. Experimental apparatus

The simplest and most successful apparatus consisted of the sample being mounted inside a massive copper block immersed in liquid helium with connections for four-terminal resistive measurements. In order to reduce the external noise, all the connections to the room temperature were made through 500-Ω resistors cooled at helium temperature. Moreover, the amplifiers and the sweep generator were battery powered. Since the stability of the external conditions during the time of a particular distribution measurement is very important, efforts were made to reduce small drifts of electronics.

The bath temperature was controlled by the stabilization of the helium pressure and by the current through a heater in the bath which was controlled by a feedback circuit connected to a germanium thermometer. Since no variation on the thermometer resistance was observed during the time of a distribution measurement (~ 3 min) any occasional temperature drift was less than 1 mK.

In Fig. 1, a block diagram of the electronics setup is shown. The current generator biased the junction through a 100-kΩ limiting resistor using a trapezoidal-shaped waveform (see Fig. 1) at a frequency of about 50 Hz. The current to the junction also passed through a high precision resistor whose voltage was amplified and sent to the trigger of a pulse generator. The 20 μs width pulse from this generator was synchronized with the sharp rise of the current ramp, and provided the trigger for the multichannel analyzer (NS-570A Tracor Northern).

The junction voltage was amplified and sent to the trigger of a second pulse generator which provided a pulse at the time of the switching to the $V\neq 0$ state. This 20 μs width pulse was sent to the stop-time input of the analyzer and a count is therefore assigned in the channel corresponding to the time t. About 10^4 events of this kind were measured and recorded, in a period of about 3 min, to get a distribution of counts versus channel number, which formed the experimental hystogram equivalent of $P(t)$. The time resolution was 20 μs (width of one channel) while the maximum number of channels available in the analyzer was 1016.

The current resolution, as well as the width in channels of the distribution, depends on the slope of the linear part of the bias current ramp. This slope ($\simeq 2$ nA/μs) was adjusted in order to have a current resolution of $\simeq 40$ nA/channel, and distributions 40–60 channels wide (tail included). Good statistics for such distributions can be obtained in about 3 min (~ 700–800 events/channel at the maxima; 5 counts/channel in the tail). Counting for too long was avoided to reduce the effect of small drift of the external conditions.

C. Calibration

The described apparatus provides the hystogram $P_c(N)$ of the counts versus the channel number N, which is equivalent to $P(t)$. For a valid comparison with theory, a careful calibration has to be made. After the

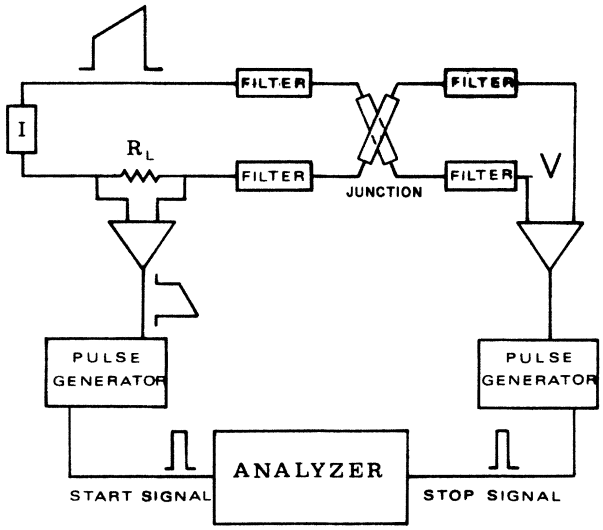

FIG. 1. Block sketch of the electronics setup. The filters are close to the junction in the liquid-helium bath.

measurement, the current ramp has been visualized on the analyzer with the same time scale of the distribution (i.e., the channels scale). This can be obtained by switching the input of the analyzer to the voltage across the current resistor. The multichannel analyzer then measured the number of counts in each channel, C_N, which are proportional to the bias current at the time corresponding to N. The coefficients C_0 and b of the trapezoidal current ramp, where $I=A(C_0+bN)$, can now be determined with high precision (to better than $\pm 0.1\%$). The proportionality constant A between the current and the counts (which finally allows the calibration of the channel number in terms of I), was already determined (to $\pm 1\%$) by supplying a known current through the current resistor in the actual measuring setup. Therefore, the final expression for the calibration of the channel number in terms of current is determined to $\pm 1\%$ because of the uncertainty in the determination of A. However, the ratio of currents in different channels is known much better since it depends only on C_0 and b. For this reason relative values of the dimensionless bias parameter $\alpha=I/I_c$, whose calibration allows the comparison with theory, can be determined to better than $\pm 0.1\%$. Note that while the critical current I_c is typically taken as a free parameter, it is actually the channel number, N_c, which is determined.

Performing the fittings in terms of $P(t)$, instead of τ, has the advantage that the statistical error on the data is well known, being given by Poisson statistics. Moreover, some other possible sources of errors have been checked. For the total time (~ 3 h) of the distribution set measurements, the waveform of the bias current generator was never changed. However, the calibration was made after each distribution record in order to estimate even small drift of the electronics setup. No variations of b were observed whereas a systematic decrease of C_0 was observed, indicating a small current drift (15 nA/min) or 1% per hour. The smearing, which comes from such a drift, is unimportant in our measurements of the distributions since it corresponds to only one channel drift in our 3-min runs.

Finally, in order to calibrate the time resolution of our apparatus, a second, synchronized 20 μs width pulse with a fixed delay time was applied to the input. Instead of a single channel populated, we found a Gaussian-like distribution with half width $\sigma \simeq 1.5$ channels. The resulting small error on the time axis has been taken into account in performing the fittings of the experimental distributions, although it produces only small variations on the χ^2 tests.

IV. ANALYSIS

Figures 2(a) and 2(b) show the data taken at various temperatures, plotted as $P(\alpha)$ versus α; the theoretical curves are calculated using the refined treatment of Kramer's low damping theory discussed in Ref. 9, which provides a complete description of extremely underdamped junctions. As a general consideration we notice that all the distributions have a characteristic asymmetry with an almost exponential tail at low current and a more abrupt cutoff at high I.

The best fittings are made by χ^2 tests, i.e., we have looked for the free-parameter values in the theory which minimize the χ^2 variable defined as

$$\chi^2=\sum_i (P_i-P_{\text{theor}})^2/\sigma_i^2 ,$$

where P_i and P_{theor} are, respectively, the experimental and the theoretical distributions and σ_i is statistical error on P_i. For χ^2 minimization we used the multivariables minimization program which provides the best fitting parameters, the best χ^2 value and the covariance matrix. As is well known, the χ^2 value provides a good test to check the statistical compatibility of experiments with theory. The free parameters in the theory are the critical current I_c (actually the corresponding channel N_c, as above described), the effective resistance in the RSJ model, and an effective noise temperature T_N which induces thermal as well as external electrical noise. Although considerations similar to those of Ref. 26 ensured that neither low-frequency noise [which would smear out $P(I)$ to approach a Gaussian distribution], nor external transients (distributions independent of I at low I) influenced the switching, we made a first series of fittings taking the temperature as a free parameter to ex-

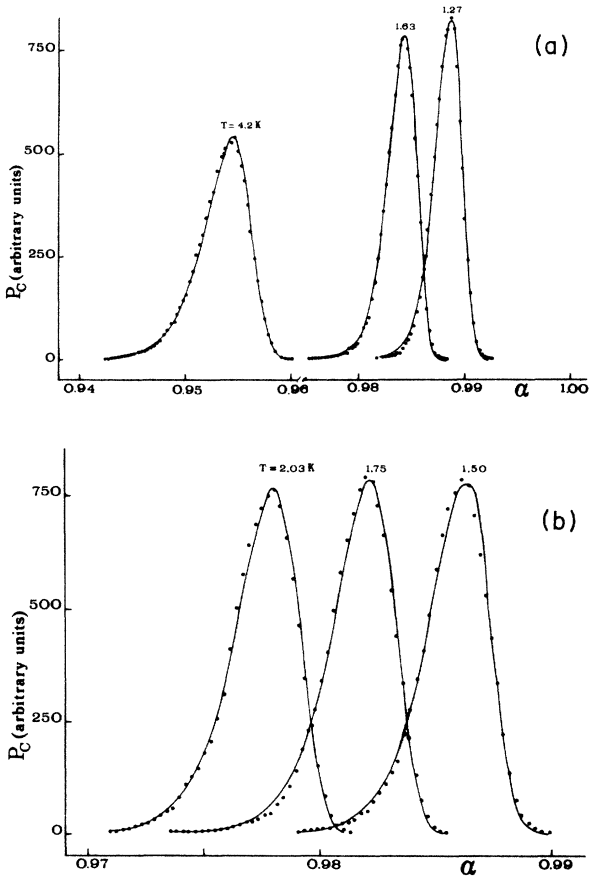

FIG. 2. Experimental distributions (solid circles) taken at indicated temperatures plotted as P_c vs α. The solid lines are the theoretical curves calculated using Ref. 9 and from the two-parameter fit reported in Table I.

TABLE I. Results of the analysis based on three χ^2 tests. For each test we report the values of the free parameters determined by minimizing χ^2. The accumulated χ^2 values divided by the degrees of freedom, N, are shown in the last columns.

Three parameters					Two parameters $T_N=T$			One parameter $T_N=T$, $I_c=165.00$ μA	
T (K)	T_N (K)	I_c (μA)	R (Ω)	χ^2/N	I_c (μA)	R (Ω)	χ^2/N	R (Ω)	χ^2/N
2.03	1.980	164.962	21.81	37.9/35	165.123	14.25	39.6/36	24.82	43.4/37
1.83	1.810	165.130	15.84	37.4/41	165.290	13.86	38.1/42	39.56	55.7/43
1.75	1.743	164.923	58.2	45.7/42	164.886	72.12	46.7/43	40.10	49.2/44
1.63	1.623	165.011	211.0	52.0/46	165.016	216.6	52.3/47	230.4	52.4/48
1.50	1.539	164.960	318.5	31.0/39	164.840	460.6	31.5/40	211.4	42.7/41
1.27	1.273	164.928	810.1	61.0/38	164.886	993.0	61.4/39	548.0	71.9/40
4.2	4.197	144.69	1.087	30.0/55	144.69	1.113	30.1/56		

perimentally verify that no external noise (which would produce actual fit temperature higher than the bath temperature) affected our experiments. The results of three different fittings are summarized in Table I.

In a first series of fittings we left free the three parameters T, I_c, and R. We notice that the χ^2 values show statistical compatibility between theoretical and experimental distributions. Moreover, the fit temperatures are fluctuating around the actual measured temperatures with very small deviations (the maximum deviation is 0.05 K) showing good agreement of the noise temperature with the bath temperature.

For a further investigation of this important point, we made a second series of fits fixing the temperature to the bath temperature and leaving free I_c and R. We notice that the quality of fits is no worse; this means that the temperature is not really a free parameter, and thus provides proof that no external noise is present.

The fit resistances R show a clear temperature dependence as shown in Fig. 3. The error bars for R have been estimated by analyzing the fluctuations of R which do not produce substantial changes in the quality of the fits within statistically allowed fluctuations of the other parameters. In fact, we observe correlations between the fit parameters. These correlations do not greatly affect the determination of I_c and T_N, but they lead to a somewhat poorer determination of R. Examples of the fluctuations of R with small variations of T_N and I_c are represented by the three series of fittings reported in Table I; the error bars in Fig. 3 include these fluctuations. We notice, however, that in spite of these fluctuations the temperature dependence of R is well characterized.[34]

The semilogarithmic plot of R versus T^{-1} emphasizes the exponential behavior which is typical of a subgap junction resistance, $R\alpha\exp(\Delta/k_BT)$, corresponding to the thermal activation of quasiparticles over the superconductor energy gap Δ. A comparison with two subgap resistances measured on the I-V characteristics at voltages of 300 and 30 μV is also shown. We notice for the fit resistance almost the same slope of the 30 and 300 μV resistances before they saturate. However, the effective resistance value is lower than the lowest quasiparticle resistance measured on the I-V characteristic close to the origin (down to 5 μV). We have no model to explain such a difference; additional theoretical and experimental work is needed to understand this result.

Devoret *et al.*[28] have established that the effective damping resistance should be evaluated at the plasma frequency, $\bar{\omega}$, and that in this range of frequencies ($\sim$GHz), external elements to the junction can affect R. Our blocking resistors were metal-film type and connected to the junction with a short (several cm long) 0.007-in.-diam Cu wire. Although frequency dependent losses in this "transmission line" could account for some of the temperature variation of R, it is unlikely to explain the three orders of magnitude change in R with temperature, when $\bar{\omega}$ changes by only a factor of about 2 over the same range of T.

Note also that the drop of I_c to $\sim$145 μA at 4.2 K is reasonably consistent with experimental determinations[35] of $I_c(T)$ made on other superconductors.

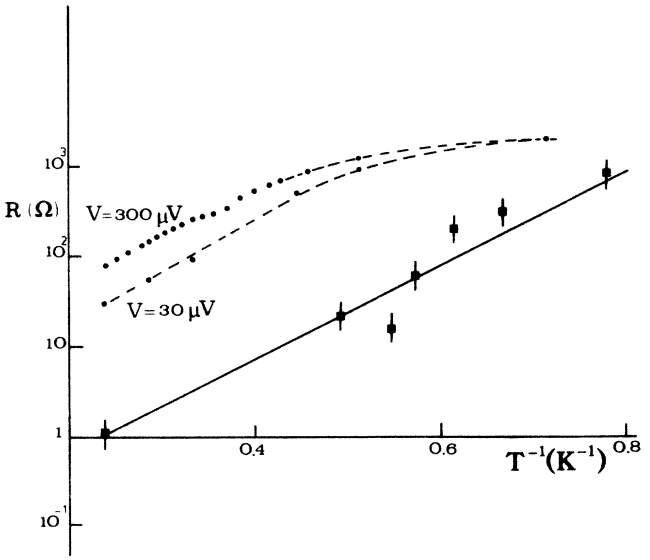

FIG. 3. Some typical junction resistances plotted vs T^{-1}: Curves are the dynamical subgap resistances taken at $V=300$ μV and $V=30$ μV, respectively; the solid squares are the effective junction resistance values obtained by the three-parameter fit to the data (see Table I). The effective junction resistance follows $R=R_0\exp(\Delta/k_BT)$ with $R_0=5.75\times10^{-2}$ Ω and $\Delta=1.1$ meV.

Finally, we notice that, in agreement with the theoretical I_c versus T dependence, the fit values of I_c are found to be approximately constant at low temperatures ($T \leq 2.03$ K), with fluctuations of about $\pm 0.1\%$ around a common value. Therefore, we have also fit with the effective junction resistance the only free parameter, by also fixing I_c to the average value obtained in the previous series of fittings (i.e., 165.00 μA). In this case the fits were somewhat poorer, indicating how sensitive the fits are to small variations of I_c. At first sight this seems wrong, since physically I_c must have at most a very small and monotonic variation with T. However, this result can be understood by realizing that the I_c used in the fit must be allowed to seek its most suitable value which is consistent with the uncertainty ($\sim 0.1\%$) in the current calibration through C_0 and b. Thus more precise R values cannot be obtained by fixing I_c unless a more precise calibration procedure for currents can be implemented.

We want to point out that in the light of these fittings the assumption of the extremely low damping framework for our experiment is verified. In fact the ratio τ_{TR}/τ_{LD} is significantly less than one (10^{-1}–10^{-3}) for all the experimental distributions except that at $T=4.2$ K, which is actually very close to the crossover point between the region of validity of the transition rate theory and the very low damping theory ($\tau_{TR} \simeq \tau_{LD}$).

Anyway, we made an attempt to fit the distributions within the transition rate theory picture. As expected, the $T=4.2$ K distribution can be fit in this framework as well as in that of the very low damping theory, resulting in $T_N \cong 4.2$ K, as the fit temperature. However, at lower temperature and increasing resistance, the transition rate theory starts failing and no statistical compatibility between data and theory can be obtained, except for some qualitative agreement due to the typical exponential behavior of $\tau(I)$ in all the theories.

V. CONCLUSION

Switching-current-distribution measurements in an extremely hysteretic Josephson junction at various temperatures are presented. A careful fitting of the data provides an experimental check of the thermal activation theory in the very low damping limit. Moreover, the fittings show that no external noise affects our measurements and allow us to obtain as a fit parameter the effective resistance of a Josephson tunnel junction in the RSJ model.

Although the correlation between the fit parameters does not allow us to get a very precise determination of R at each temperature, R shows a well-defined behavior as a function of the temperature. In fact R has the typical temperature dependence of a subgap resistance, $R \propto \exp(\Delta/k_B T)$, but it is lower than the dc resistance measured on the I-V curve at low voltage (down to 5 μV).

Moreover, we have shown in this work that very careful fittings have to be performed on switching distribution measurements in order to get useful information. Indeed a qualitative agreement between experiments and theory is often obtained very easily because of the typical, almost exponential behavior of $\tau(I)$ in all the damping regimes.

ACKNOWLEDGMENTS

We would like to thank Maurizio Russo, who supplied us with the junction, as well as Roberto Cristiano and Sergio Pagano for useful discussions and suggestions. This work was supported in part by the Istituto Nazionale Fisica Nucleare, Napoli, and the U.S. Department of Energy, Basic Energy Sciences-Materials Sciences, under Contract No. W-31-109-ENG-38.

*Present address: 1253 Vandoeuver, Switzerland.

[1] V. Ambegaokar and B. I. Halperin, Phys. Rev. Lett. **22**, 1364 (1969).
[2] P. A. Lee, J. Appl. Phys. **42**, 325 (1971).
[3] J. Kurkijarvi, Phys. Rev. B **6**, 832 (1972).
[4] H. D. Vollmer and H. Risken, Z. Phys. B **37**, 343 (1980), and references of the same authors reported therein.
[5] P. B. Visscher, Phys. Rev. B **13**, 3272 (1976).
[6] P. B. Visscher, Phys. Rev. B **14**, 347 (1976).
[7] B. Carmeli and A. Nitzan, Phys. Rev. Lett. **51**, 233 (1983).
[8] M. Buttiker, E. P. Harris, and R. Landauer, Phys. Rev. B **28**, 1268 (1983); M. Buttiker and R. Landauer, *ibid.* **30**, 1551 (1984).
[9] A. Barone, R. Cristiano, and P. Silvestrini, J. Appl. Phys. **58**, 3822 (1985).
[10] R. Cristiano and P. Silvestrini, J. Appl. Phys. **60**, 3243 (1986).
[11] Yu. N. Ovchinnikov, R. Cristiano, and A. Barone, J. Appl. Phys. **56**, 1473 (1984).
[12] A. Barone and Y. N. Ovchinnikov, J. Low Temp. Phys. **55**, 297 (1984).
[13] A. O. Caldeira and A. J. Leggett, Phys. Rev. Lett. **46**, 211 (1981).
[14] A. J. Leggett, Phys. Rev. B **30**, 1208 (1984).
[15] L. D. Chang and S. Chakravarty, Phys. Rev. B **29**, 130 (1984).
[16] V. Ambegaokar, V. Eckern, and G. Shön, Phys. Rev. Lett. **48**, 1945 (1982).
[17] H. Grabert, V. Weiss, and P. Hanggi, Phys. Rev. Lett. **52**, 2193 (1982).
[18] A. Larkin and Y. N. Ovchinnikov, in *Josephson Effect—Achievements and Trends,* edited by A. Barone (World-Scientific, Singapore 1986), pp. 18–33.
[19] V. I. Mel'nikov, Physica **130A**, 606 (1985).
[20] J. T. Anderson and A. M. Goldman, Physica **55**, 256 (1971).
[21] T. A. Fulton and L. N. Dunkleberger, Phys. Rev. B **9**, 9760 (1974).
[22] L. D. Jackel, W. W. Webb, J. E. Lukens, and S. S. Pei, Phys. Rev. B **9**, 115 (1974).
[23] C. M. Falco, W. H. Parker, S. E. Trullinger, and P. K. Hansma, Phys. Rev. B **10**, 1865 (1974).
[24] J. Clarke and G. Hawkins, Phys. Rev. B **14**, 2826 (1976).
[25] R. F. Voss and R. A. Webb, Phys. Rev. Lett. **47**, 265 (1981); S. Washburn, R. A. Webb, R. F. Voss, and S. Faris, *ibid.* **54**, 2712 (1985).

[26]L. D. Jackel, J. P. Gordon, E. L. Hu, R. E. Howard, L. A. Fetter, D. M. Tennant, R. W. Epworth, and J. Kurkijarvi, Phys. Rev. Lett. **47**, 697 (1981); M. H. Devoret, J. M. Martinis, and J. Clarke, *ibid.* **55**, 1908 (1985).

[27]R. H. Kock, D. J. Van Harlingen, and J. Clarke, Phys. Rev. B **26**, 74 (1982).

[28]M. H. Devoret, J. M. Martinis, D. Esteve, and J. Clarke, Phys. Rev. Lett. **53**, 1260 (1984).

[29]W. C. Danchi, J. B. Hansen, M. Octavio, F. Habbal, and M. Tinkham, Phys. Rev. B **30**, 2503 (1984).

[30]H. Akoh, O. Liengme, M. Iansiti, M. Tinkham, and J. V. Frec, Phys. Rev. B **33**, 2038 (1986).

[31]R. F. Miracky, M. H. Devoret, and J. Clarke, Phys. Rev. A **31**, 2509 (1985).

[32]J. Clarke, M. H. Devoret, J. Martinis, and D. Esteve, in *Josephson Effect—Achievements and Trends*, edited by A. Barone (World- Scientific, Singapore, 1986), p. 17.

[33]H. A. Kramers, Physica **7**, 284 (1940).

[34]Such typical subgap resistances are the parallel combination of the quasiparticle temperature-dependent resistance and the temperature-independent leak resistance R_L, which causes the saturation at low temperature. Such saturation value is 2500 Ω. Because of this rather high R_L value, no saturation is observed in the fit resistance.

[35]See, e.g., L. Solymar, *Superconductive Tunneling and Applications* (Wiley, London, 1972), p. 152.